

# Aqueous Methane in Slit-Shaped Silica Nanopores: High Solubility and Traces of Hydrates

Anh Phan<sup>#</sup>, David R. Cole<sup>+</sup>, and Alberto Striolo<sup>#,\*</sup>

<sup>#</sup> University College London, Department of Chemical Engineering, Torrington Place, London, WC1E7JE, United Kingdom

<sup>+</sup>School of Earth Sciences, The Ohio State University, Columbus, Ohio 43210, USA

## Supplemental Material

### Algorithms

1. Algorithm to calculate density profiles for confined methane molecules in the direction perpendicular to the methane – water interface.

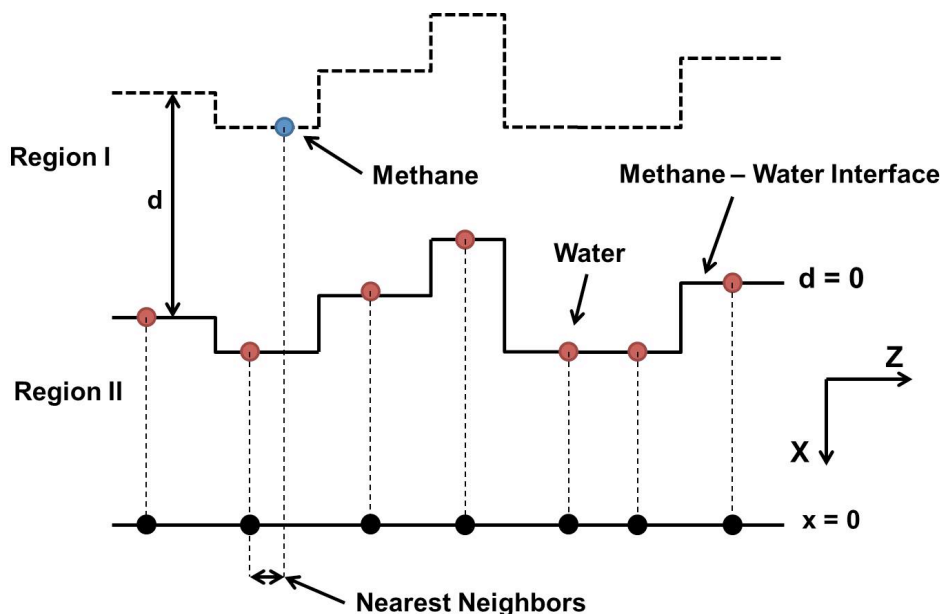


**Figure S1.** Schematic diagram describing the algorithm for the calculation of the distance of a methane molecule from a rugged methane – water interface.

Implementing the algorithm proposed Berkowitz et al.<sup>1</sup>, we calculated the perpendicular distance  $d$  between one methane molecule in Region I and II and the rough methane – water interface through these steps:

- a. The coordinates of the water oxygen atoms at the interface are projected onto the  $X = 0$  plane.
- b. The coordinates of the methane molecules are projected onto the  $X = 0$  plane.
- c. A methane molecule is associated with the closest water oxygen atom at the interface.

- d. The distance  $d$  perpendicular from the rough interface is the distance between the X coordinate of the methane molecule and that of its associated water oxygen atom.

## 2. Methane solubility in liquid water

The methane solubility in water in Region I is defined as the ratio of the density of CH<sub>4</sub> molecules in the direction perpendicular to the methane/water interface as Figure 2 ( $d = \sim 29$  to  $\sim 15$  Å) to the density of water oxygen atoms in the X direction through silica pore, as shown in Figure S2 ( $x = 15$  to  $29$  Å). The following equation is used:

$$CH_4 \text{ Solubility} \times 10^3 = \frac{\langle \rho_{CH_4} \rangle}{\langle \rho_{H_2O} \rangle_{Region I}} \times 10^3$$

## 3. Pressure tensor in the pore

To evaluate the local pressure tensor inside the slit-pore, we calculated the local tangential component of the pressure tensor  $P_{xx}$  perpendicular to the methane-water interface. We conducted these calculations in the region ‘deep’ into the pore, far from both the pore-bulk and methane-water interfaces. The following equation is derived by Walton et al.<sup>2</sup> for an infinite interface in the x-y plane:

$$P_{xx} = P_{T,IK}(z) = \rho(z)k_B T - \frac{1}{4A} \left\langle \sum_{i,j} \frac{x_{ij}^2 + y_{ij}^2}{r_{ij}} \frac{1}{|z_{ij}|} \frac{du(r_{ij})}{dr_{ij}} \times \theta\left(\frac{z - z_i}{z_{ij}}\right) \theta\left(\frac{z_j - z}{z_{ij}}\right) \right\rangle$$

In this equation  $A$  is the surface area within which averages are computed,  $\theta(x)$  is the unit step function, and  $x_{ij}$ ,  $y_{ij}$ ,  $z_{ij}$  are components of the intermolecular separation vector  $r_{ij}$ . We computed the pressure tensor every 0.1 Å along the z-axis of the slit-pore. We point out that Long et al.<sup>3</sup> recently employed this method for calculating the pressure tensor for argon within slit-shaped carbon pores.

## 4. Excess chemical potential

Initially, we conducted simulations at 300 K for bulk liquid water and liquid water confined in the silica pore without methane to create configurations for the Widom insertion method.<sup>4</sup> In the Widom insertion method, after inserting a methane molecule at a random position in the systems, we calculated  $\exp(-\beta\Delta U)$ , where  $\Delta U$  is the potential energy difference between the systems before and after adding a CH<sub>4</sub> molecule,  $\Delta U = U(N_{tot} + N_{CH_4}) - U(N_{tot})$ , with  $N_{CH_4} = 1$ . The excess chemical potential is an average over all the configurations, defined as:

$$\Delta\mu_{ex} = -kT \ln \frac{\langle V \int ds_{N+1} \exp(-\beta\Delta U) \rangle}{\langle V \rangle}$$

In the prior equation  $k$  is the Boltzmann constant,  $T$  is the absolute temperature of the system,  $\beta = 1/kT$ ,  $V$  is the volume of the system, and  $\langle \dots \rangle$  indicates an ensemble average.

#### 5. F4 structural order parameter

The F4 structural order parameter developed by Rodger et al.<sup>5</sup> is used to describe the local arrangement of water molecules at different positions during our simulations. The F4 order parameter is based on the H-O...O-H torsion angle,  $\phi$ , for two next-neighboring water molecules:

$$F_4 = \langle \cos 3\phi \rangle$$

In this equation  $\phi$  is the dihedral angle between the vector OH of a given water molecule and the vector OH of another water molecule found within 3.5 Å from the first water molecule.<sup>6</sup> Note that all the water molecules considered for this calculation are found within 5.45 Å from a methane molecule (they belong to the methane hydration shell). The hydrogens considered are the outer-most ones for each water dimer. The distance of 3.5 Å is consistent with the first minimum in the water oxygen – water oxygen radial distribution functions  $g_{OO}(r)$  in liquid water.<sup>7</sup> The order parameters were obtained as average over all possible angles correlated with a given water, and then over all water molecules in a hydration shell.

## Results

### 1. Water density profiles in the X direction inside the pore

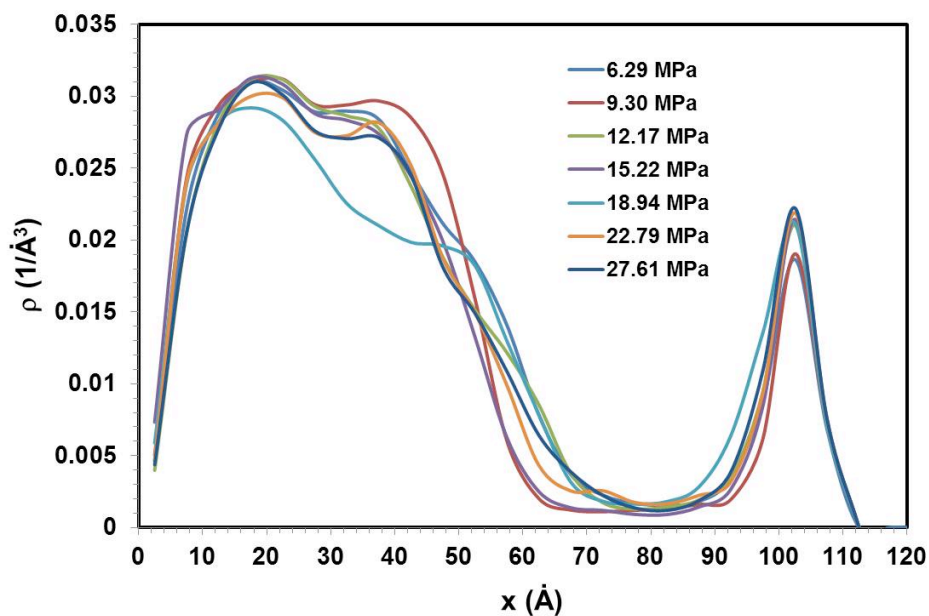


**Figure S2.** Density profiles of water oxygen atoms as a function of distance  $x$  through the silica pore. The results are obtained from seven simulation systems. The reference ( $x=0$ ) is the plane located at the position of the pore entrance (left side).

In Figure S2, we report the results of water oxygen density profiles as a function of distance  $x$  through the silica pore when the bulk pressure increases. The reference ( $x = 0$ ) corresponds to the plane located at the pore entrance (left side). The results in Figure S2 indicate that generally the increase of the bulk pressure of the system does not impact the structural properties of water molecules.

## 2. Pressure Tensor in the Pore

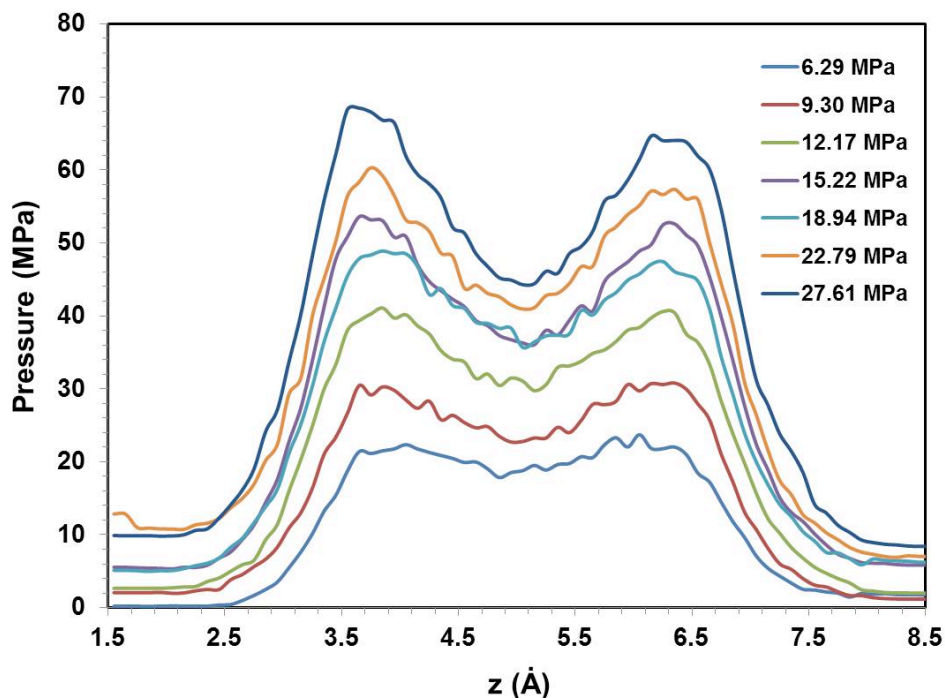


**Figure S3.** Tangential pressure tensor profiles for seven methane-water systems confined in the silica pore at 300K.

In Figure S3, the results for tangential pressure tensor  $P_{xx}$  as a function of the distance  $z$  across the silica pore are shown for seven simulated systems. Generally, as the bulk pressure increases, the tangential pressure tensor  $P_{xx}$  inside the pore also increases. Our results show that, unexpectedly, as the bulk pressure increases from 18.94 to 22.79 MPa, the tangential pressure tensor  $P_{xx}$  decreases slightly.

## 3. Excess Chemical Potential

In Table S1 we report the results of the excess chemical potential for methane in bulk liquid water and in confined liquid water. Our calculations in bulk water are in good agreement with literature simulation data.<sup>4,8</sup> Our data show that the excess free energy for methane in bulk liquid water is higher than that for methane in confined liquid water, which is consistent with higher solubility predicted for methane in confined versus in bulk water.

**Table S1.** Excess chemical potential for methane in bulk and confined liquid water at 300K.

System	Excess Chemical Potential ( kJ/mol)
CH <sub>4</sub> in Bulk Water	9.31
CH <sub>4</sub> in Water confined in SiO <sub>2</sub> Pore	8.77

## References

- (1) Pandit, S. A.; Bostick, D.; Berkowitz, M. L. An algorithm to describe molecular scale rugged surfaces and its application to the study of a water/lipid bilayer interface. *J. Chem. Phys.* **2003**, 119, 2199-2205.
- (2) Walton, J. P. R. B.; Tildesley, D. J.; Rowlinson, J. S.; Henderson, J. R.; The Pressure Tensor at The Planar Surface of a Liquid ,*Mol. Phys.* **1983**, 48, 1357–1368.
- (3) Long, Y.; Palmer, J. C.; Coasne, B.; Sliwinski-Bartkowiak, M.; Gubbins, K. E. Pressure enhancement in carbon nanopores: a major confinement effect. *Phys. Chem. Chem. Phys.* **2011**, 13, 17163-17170.
- (4) Lee, J.; Aluru, N. R. Water-solubility-driven separation of gases using graphene membrane. *J. Membrane Sci.* **2013**, 428, 546-553.
- (5) Rodger, P. M.; Forester, T. R.; Smith, W. Simulations of the methane hydrate methane gas interface near hydrate forming conditions. *Fluid Phase Equilib* **1996**, 116, 326-332.
- (6) Liang, S.; Kusalik, P. G. Exploring nucleation of H<sub>2</sub>S hydrates. *Chem. Sci.* **2011**, 2, 1286-1292.
- (7) Bagherzadeh, S. A.; Englezos, P.; Alavi, S.; Ripmeester, J. A. Influence of Hydrated Silica Surfaces on Interfacial Water in the Presence of Clathrate Hydrate Forming Gases. *J Phys Chem C* **2012**, 116, 24907-24915.
- (8) Konrad, O.; Lankau, T. Solubility of methane in water: The significance of the methane-water interaction potential. *Journal of Physical Chemistry B* **2005**, 109, 23596-23604.